Kossel Line Analysis on Colloidal Crystals in Semidilute Aqueous Solutions

Tsuyoshi Yoshiyama and Ikuo Sogami
Department of Physics, Kyoto Sangyo University, Kyoto 603, Japan

and

Norio Ise
Department of Polymer Chemistry, Kyoto University, Kyoto 606, Japan
(Received 23 July 1984)

An analysis of Kossel lines is reported for colloidal crystals of highly charged polystyrene particles in semidilute aqueous solutions. The phase transformation between fcc and bcc structures and their coexistence is observed. Lattice constants are found to be systematically smaller than those calculated from the uniform particle distribution throughout solution. This observation shows that a long-range weak attraction also exists between colloidal particles. The fine structure of the Kossel line is explained by use of dynamical theory.

PACS numbers: 61.50.Cj, 61.14.Fe, 82.70.Dd

Aqueous suspensions of monodisperse, charged, polystyrene particles exhibit crystalline orderings. Properties of these colloidal crystals which have, typically, lattice spacings of the order of visible-light wavelengths have been investigated by optical diffraction methods[1-4] and by means of optical microscopes.[5,6] By adjusting the conditions such as the radius, surface-charge density, concentration of particles, salt concentration, and temperature, it is possible to control the properties of colloidal crystals over a wide range. This is perhaps the most essential characteristic of colloidal crystals which has no counterpart in atomic crystals. In this note, we report the results of a Kossel line analysis and systematic investigations of the particle-concentration dependence of crystal structures and lattice constants of polystyrene crystallites in semidilute aqueous solutions.

Kossel lines of colloidal crystals were first observed in dilute solutions and interpreted as the indicator of crystal perfection by Clark, Hurd, and Ackerson.[3] Pieranski *et al.*[4] emphasized the importance of Kossel line analysis in the determination of crystal structures. The Kossel images viewed by both of them are, precisely speaking, *pseudo-Kossel images,*[7] because they used a divergent beam technique, i.e., they placed a thin sheet of scatterer outside the solution container to make a point light source. In our experiments, however, we observed faint light signals of backward diffraction patterns from lattice planes illuminated by divergent beams which were produced at a point source existing intrinsically inside colloidal crystallites. In this sense the diffraction images observed in our experiment are optical analogs of the *intrinsic Kossel images* of atomic crystals by x-rays, an elegant analysis of which was made by Laue[8] with the aid of the law of reciprocity. Following Laue's viewpoint, we analyze the geometrical and dynamical aspects of the intrinsic Kossel images of colloidal crystallites without being confronted by complicated refraction effects due to incident divergent beams from outside crystal.

Latex solutions of surphonate-modified polystyrene particles (diameter 1560 Å and surface charge -3×10^4e determined by titration) were deionized by anion and cation ion-exchange resins until the suspensions showed irridescence, and then introduced into rectangular quartz cuvettes of dimension 1 mm×10 mm×40 mm. With use of He-Ne and Ar laser beams, optical diffraction experiments on colloidal crystals were made over the particle concentration range from 9.8 to 0.6 vol%. Backward diffraction spots and Kossel images were photographed on Fuji FG film with a modified rotating-crystal camera consisting of a cylindrical film holder with diameter 5.37 mm, a collimation slit of 1 mm diameter, and a goniometer head on which the specimen cuvette is mounted. In order to decrease diffuse-reflection noise and crystal disturbances by the incident laser beam to as low a level as possible, we used laser-beam sources with low power (2 mW He-Ne and 5 mW Ar). All data analyzed here are diffraction signals from the middle part of the cuvette; variation due to sedimentation has been estimated as less than a few percent.

If the specimens remained motionless, the crystallites gradually grew into larger gains in dilute solutions; concentrated solutions were filled rather rapidly with a large number of tiny crystallites which did not grow further. Very clear Kossel images could be observed when the crystal grains had grown to considerable size in the dilute solutions. The signals of such clear Kossel images, however,

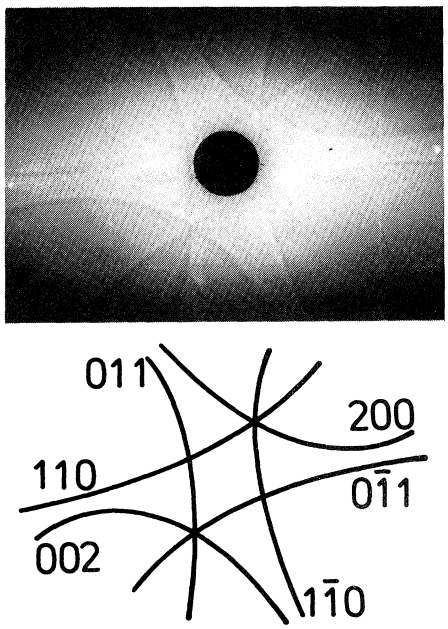

FIG. 1. Backward Kossel images with dark and bright fine structure from a colloidal crystal in polystyrene latex solution (1.5 vol%). The indices of the Kossel rings show that the crystal structure is bcc and the incident direction of the laser beam is [101].

became faint and sometimes disappeared when the crystallites had grown into larger single crystals. These facts indicate that the appearance of Kossel imates requires a moderate degree of perfection of the crystallites, and that the origin of the point source of the divergent beams is deeply related to the degree of imperfection of the crystallites. Direct observation by microscope readily demonstrates the existence of defects such as dislocations and vacancies in moderately perfect crystallites. Accordingly, it is natural to interpret the point source of divergent beams as being provided by such a defect inside the crystallite, where the incident beams are randomly scattered.

An example of Kossel lines of colloidal crystals and their indexings is shown in Fig. 1 for a 1.5-vol% sample. This crystal structure is bcc, and the Kossel lines have dark and bright fine structure. By indexing the Kossel lines of a series of samples with different latex concentrations, we found that the crystal structure transforms from fcc at high concentration (> 3.5 vol%) to bcc at low concentrations (< 2.5 vol%). In the transition region (2.5–3.5 vol%) where crystallites with bcc structure and fcc structure coexist, twin formation and the appearance of the body-centered tetragonal structure were recognized.

The variation of the size and relative position of Kossel rings versus latex concentration is shown in Fig. 2. In this figure, we see that the width of the Kossel lines is broad in the concentrated specimen and sharpens gradually with decreasing latex concentration. Interplanar distances are determined, after correction for the refractive index, from measurements of the radii of the Kossel rings. Some of the lattice constants thus obtained for different values of the volume fraction ϕ in solution are given in Table I. Lattice constants determined from the Debye-Scherrer rings, which were observed at the initial polycrystalline stages for dilute specimens, are also listed for comparison. The center-to-center interparticle distance R is calculable from

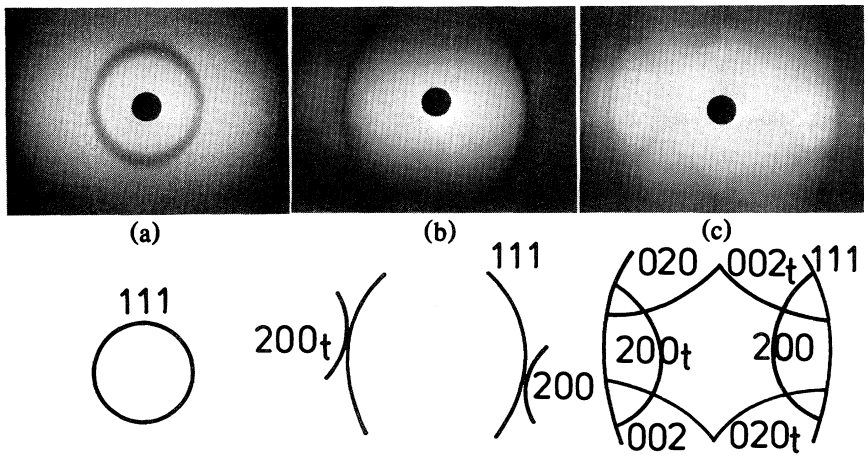

FIG. 2. Variation of the 111 backward Kossel rings of fcc crystal upon dilution. (a) 6.0 vol%, the ring has the line width $\Delta\alpha = 4.7°$; (b) 4.0 vol%, the 200 Kossel ring touches on the 111 Kossel ring when the lattice constant is $a_0 = 5105$ Å; (c) 3.0 vol%, the indices with subscript t show the twin ring.

TABLE I. Crystal structures and lattice constants a_K and a_{DS} determined, respectively, from Kossel rings and Debye-Scherrer rings.

100ϕ	Structure	a_K (Å)	a_{DS} (Å)
0.6	bcc	7118 ± 70	7248 ± 20
0.8	bcc	6705 ± 30	6759 ± 30
1.0	bcc	6025 ± 100	6283 ± 40
2.0	bcc	4939 ± 60	4875 ± 80
3.0	fcc	5542 ± 50	5552 ± 10
4.0	fcc	4965 ± 100	
6.0	fcc	4344 ± 70	
8.0	fcc	4141 ± 30	
9.8	fcc	4061 ± 80	

the lattice constant if the cyrstal structure is established.

As shown in Fig. 3, the interparticle distance R in an ordered array with definite translational symmetry increases continuously as the volume fraction ϕ decreases. Notice that if the solution is filled uniformly with a crystalline distribution of latex particles, the ratio of interparticle distance R to particle radius a must obey either $R/a = 1.75/\phi^{1/3}$ for bcc structure (dashed line) or $R/a = 1.81\phi^{1/3}$ for fcc structure (dotted line). The observed values, however, are systematically smaller and are approximately on different curves, $R/a = 1.46/\phi^{1/3}$ ($0.006 \lesssim \phi \lesssim 0.035$) for bcc and $R/a = 1.57/\phi^{1/3}$ ($0.025 \lesssim \phi < 0.08$) or $R/a = 1.65/\phi^{1/3}$ ($0.08 \lesssim \phi \lesssim 0.098$) for fcc, which are drawn by solid lines. The difference between the experimental results and a uniform particle distribution amount to more than 19% (bcc), 15% (fcc, $0.025 \lesssim \phi < 0.08$), and 9.6% (fcc, $0.08 \lesssim \phi \lesssim 0.098$), while the overall experimental error is of order several percent. Hence, colloidal crystallites undergo substantial contraction in semidilute solutions.

The reduction of interparticle distance in colloidal crystals of this kind was first discovered by Ise *et al.*[6] through a detailed inspection of microscopic data. Since Kossel line analysis affords decisive information on three-dimensional crystal structures and lattice constants, the present results have made undeniable the existence of reduced spacing in colloidal crystals of highly charged particles. The effective hard-sphere model[9] with only an electrostatic repulsive potential[10] fails to explain this phenomenon. The reduction of interparticle spacing in ordered arrays, which must be compensated by increased mean interparticle distance in disordered regions, requires the existence of a long-range weak attraction in addition to the short-range

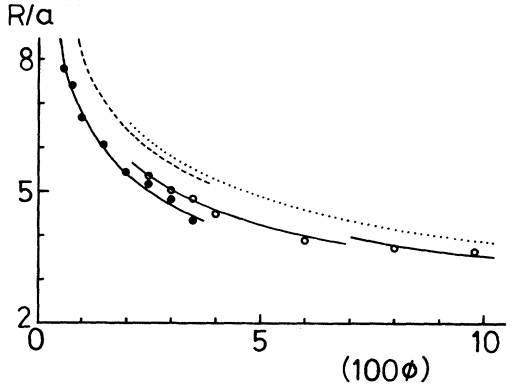

FIG. 3. Concentration dependence of the interparticle distance R. Filled circles for bcc are on $R/a = 1.46/\phi^{1/3}$ (solid line) and open circles for fcc are piecewise on $R/a = 1.57/\phi^{1/3}$ ($0.025 \lesssim \phi < 0.08$) or $R/a = 1.65/\phi^{1/3}$ ($0.08 \lesssim \phi \lesssim 0.98$) (solid lines). For comparison, curves calculated for uniform distribution of particles throughout the solution are shown by a dashed line (bcc) and a dotted line (fcc).

strong repulsion among colloidal particles. A theoretical search for the origin of such a long-range attractive force is necessary.[11]

Although the geometry of Kossel patterns is sufficient to clarify the crystallographic features of colloidal crystals, dynamical consideration is necessary to interpret the structure of individual Kossel lines. Dynamical theory[12] predicts that the width of the diffraction line satisfies

$$\Delta\alpha_h = 2\left(\frac{|\gamma_2|}{\gamma_1}\right)^{1/2}\frac{n_0|\psi_h|}{\sin 2\Theta},$$

with $\gamma_i = \cos\theta_i$ ($i = 1, 2$), where n_0 is the index of refraction, Θ is the Bragg angle at the Laue point, θ_1 (θ_2) is the angle between transmitted (diffracted) wave vector and crystal surface normal, and ψ_h is the Fourier coefficient of effective charge density in crystal. The index of refraction of colloidal crystals for visible light n_{CC} is estimated as[1]

$$n_{CC} = n_W + \Delta n_{CC} = n_W(1-\phi) + n_{PS}\phi,$$

in terms of the indices of water and polystyrene ($n_W = 1.33$ and $n_{PS} = 1.6$). The difference Δn_{CC} varies sensitively with latex concentration. On the other hand, the index of refraction of atomic crystals for x rays n_{AC} is given by $n_{AC} = 1 + \Delta n_{AC}$, and the difference Δn_{AC} (which is less sensitive to electron charge density) is measured approximately to be $\Delta n_{AC} \simeq -10^{-5}$. Since $|\psi_h|$ and $|\Delta n|$ are of the same order, the widths of diffraction lines of colloidal and atomic crystals, $\Delta\alpha_{CC}$ and $\Delta\alpha_{AC}$, satisfy roughly the relation $\Delta\alpha_{CC}/\Delta\alpha_{AC} \simeq |\Delta n_{CC}/\Delta n_{AC}|$.

This relation and the large value of the ratio $|\Delta n_{CC}/\Delta n_{AC}|$, nearly 10^3 for semidilute solutions, explains well the broad width of Kossel lines of colloidal crystals. For example, the width for NaCl 200 reflection by Cu $K\alpha$ radiation[13] is $\Delta\alpha_{AC} = 14.2''$. Therefore the width of the 111 Kossel line of colloidal crystallites, $\Delta\alpha_{CC} = 4.7°$ for $\phi = 0.06$, is reasonable. The sharpening of the Kossel line $\Delta\alpha_{CC}$ upon dilution as observed in Fig. 2 is also consistent with this interpretation.

As shown in Fig. 1, the concave and convex sides of Kossel rings are, respectively, darker and brighter than the background in a positive photograph. Fine structure of this kind was observed for all Kossel rings in the Laue case ($\gamma_2 > 0$) and for Kossel rings with a large value of $\gamma_1/|\gamma_2|$ in the Bragg case ($\gamma_2 < 0$). In the case of x-ray diffraction,[14] however, the Kossel cones have fine structure with reverse order, i.e., bright on the inside and dark on the outside in a positive photograph. Dynamical theory indicates that the contrast of line intensity against background in a positive photograph is described by C_- and C_+, respectively, just inside and outside the Kossel rings, and that $C_\pm$ are estimated approximately by[12]

$$C_\pm = 1 + \frac{\gamma_1}{|\gamma_2|} \pm 2\epsilon\left(\frac{\gamma_1}{|\gamma_2|}\right)^{1/2},$$

where ϵ is the sign of Δn. Therefore the reversal of dark and bright fine structure in Kossel lines of colloidal and atomic crystals is explained by the negative sign of the ratio $\Delta n_{CC}/\Delta n_{AC}$ which is ascribed basically to the sign of the frequency-dependent term in the dispersion formula for the index of refraction.

[1]P. A. Hiltner and I. M. Krieger, J. Phys. Chem. **73**, 2386 (1969).

[2]R. Williams and R. S. Crandall, Phys. Lett. A **48**, 225 (1974).

[3]N. A. Clark, A. Hurd, and B. J. Ackerson, Nature (London) **281**, 57 (1979); B. J. Ackerson and N. A. Clark, Phys. Rev. Lett. **46**, 123 (1981).

[4]P. Pieranski, E. Dubois-Violette, F. Rothen, and L. Strzelecki, J. Phys. (Paris) **42**, 53 (1981); P. Pieranski, Contemp. Phys. **24**, 25 (1983).

[5]S. Hachisu, Y. Kobayashi, and A. Kose, J. Colloid. Interface Sci. **42**, 342 (1973); A. Kose, M. Ozaki, K. Takano, Y. Kobayashi, and S. Hachisu, J. Colloid. Interface Sci. **44**, 330 (1973).

[6]N. Ise, T. Okubo, M. Sugiura, K. Ito, and H. J. Nolte, J. Chem. Phys. **78**, 536 (1983).

[7]H. Seemann, Ann. Phys. (Leipzig) **51**, 391 (1916), and **53**, 461 (1917), and **6**, 793 (1930), and **7**, 633 (1930).

[8]M. von Laue, Ann. Phys. (Leipzig) **23**, 705 (1935), and **28**, 528 (1937).

[9]M. Wadati and M. Toda, J. Phys. Soc. Jpn. **32**, 1147 (1972).

[10]B. V. Derjaguin, Trans. Faraday Soc. **36**, 203 (1940); E. J. W. Verwey and J. Th. G. Overbeek, *Theory of the Stability of Lyophobic Colloid* (Elsevier, Amsterdam, 1948).

[11]I. Sogami, Phys. Lett. **96A**, 199 (1983).

[12]R. W. James, *The Optical Principles of the Diffraction of X-Rays* (Bell, London, 1967).

[13]M. Renninger, Z. Kristallogr. **89**, 344 (1934).

[14]W. Kossel and H. Voges, Ann. Phys. (Leipzig) **23**, 677 (1935).

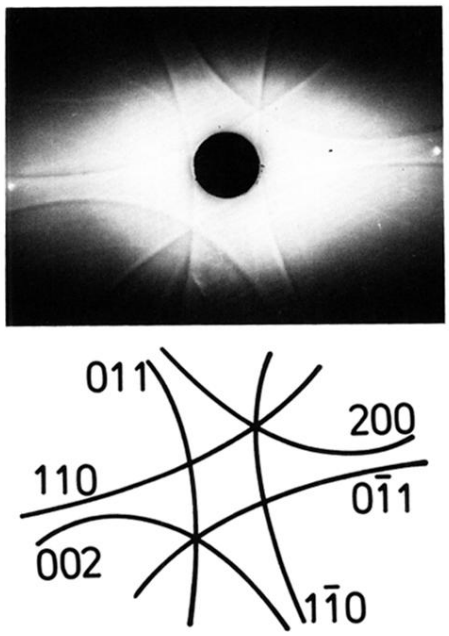

FIG. 1. Backward Kossel images with dark and bright fine structure from a colloidal crystal in polystyrene latex solution (1.5 vol%). The indices of the Kossel rings show that the crystal structure is bcc and the incident direction of the laser beam is [101].

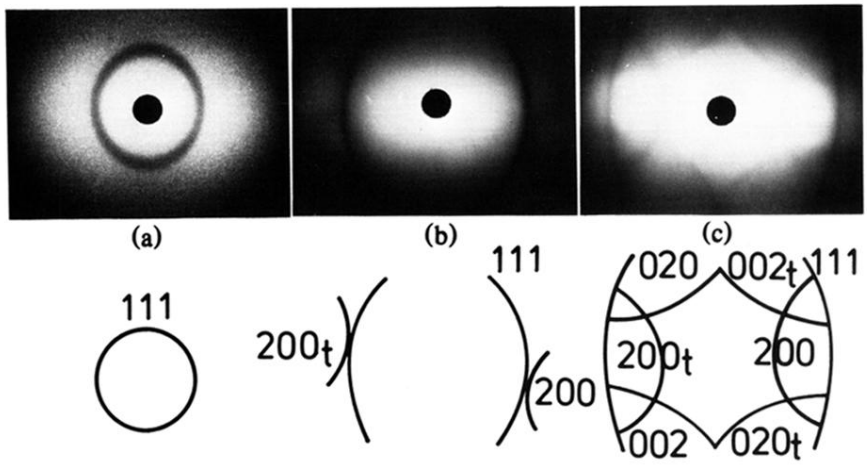

FIG. 2. Variation of the 111 backward Kossel rings of fcc crystal upon dilution. (a) 6.0 vol%, the ring has the line width $\Delta\alpha = 4.7°$; (b) 4.0 vol%, the 200 Kossel ring touches on the 111 Kossel ring when the lattice constant is $a_0 = 5105$ Å; (c) 3.0 vol%, the indices with subscript t show the twin ring.